Research Article | Vol. 25, No. 2 | 23 Jan 2017 | OPTICS EXPRESS 1598
Optics EXPRESS

Spatial-heterodyne spectrometer for transmission-Raman observations

M. J. FOSTER,* J. STOREY, AND M. A. ZENTILE

IS-Instruments Ltd, Pipers Business Centre, 220 Vale Road, Tonbridge, Kent, TN9 1SP, UK
**mfoster@is-instruments.com*

Abstract: A new transmission Raman spectrometer has been developed using a spatial heterodyne spectrometer (SHS), taking advantage of the high etendue inherent in this class of spectrometer to maximize the light collected from the target. The system has been tested against paracetamol tablet samples. The instrument has been shown to accept light from 0.05 mm up to a 3 mm core diameter fibre bundle with a numerical aperture of 0.22, whilst no degradation in resolution is observed.

OCIS codes: (120.0120) Instrumentation, measurement, and metrology; (300.0300) Spectroscopy; (280.0280) Remote sensing.

References and links

1. M. J. Pelletier, K. L. Davis, and R. A. Carpio, "Diagnostics and modeling in semiconductor manufacturing," Proceedings symposium on process control, I, Electrochemical Society, Reno, NV (1995).
2. I. M. Clegg, C. Norton, N. J. Everall, B. King, and H. Melvin, "On-Line Analysis using Raman Spectroscopy for process control during the manufacture of Titanium Dioxide," Appl. Spectrosc. **55**(9), 1138–1150 (2001).
3. Y. S. Li and J. S. Church, "Raman spectroscopy in the analysis of food and pharmaceutical nanomaterials," J. Food Drug Anal. **22**(1), 29–48 (2014).
4. J. Johansson, S. Pettersson, and S. Folestad, "Characterization of different laser irradiation methods for quantitative Raman tablet assessment," J. Pharm. Biomed. Anal. **39**(3-4), 510–516 (2005).
5. P. Matousek and A. W. Parker, "Bulk Raman analysis of pharmaceutical tablets," Appl. Spectrosc. **60**(12), 1353–1357 (2006).
6. J. Johansson, A. Sparén, O. Svensson, S. Folestad, and M. Claybourn, "Quantitative transmission Raman spectroscopy of pharmaceutical tablets and capsules," Appl. Spectrosc. **61**(11), 1211–1218 (2007).
7. M. Boiret and Y. M. Ginot, "Counterfeit detection of pharmaceutical tablets with transmission Raman spectroscopy," Spectrosc. Eur. **23**(6), 6–9 (2011).
8. T. Vigh, T. Horváthová, A. Balogh, P. L. Sóti, G. Drávavölgyi, Z. K. Nagy, and G. Marosi, "Polymer-free and polyvinylpirrolidone-based electrospun solid dosage forms for drug dissolution enhancement," Eur. J. Pharm. Sci. **49**(4), 595–602 (2013).
9. P. Matousek, N. Everall, D. Littlejohn, A. Nordon, and M. Bloomfield, "Dependence of signal on depth in transmission Raman spectroscopy," Appl. Spectrosc. **65**(7), 724–733 (2011).
10. M. J. Pelletier, P. Larkin, and M. Santangelo, "Transmission Fourier Transform Raman spectroscopy of pharmaceutical tablet cores," Appl. Spectrosc. **66**(4), 451–457 (2012).
11. J. Harlander, R. J. Reynolds, and F. L. Roesler, "Spatial Heterodyne Spectrometer for the exploration of diffuse emission line a far ultraviolet wavelengths," Astro. Phys. J. **396**, 730–740 (1992). J. M. Harlander, "Spatial heterodyne spectroscopy: interferometric performance at any wavelength without scanning," Thesis (Ph.D.) University of Wisconsin Madison (1991).
12. M. Foster, J. Storey, P. Stockwell, and D. Widdup, "Stand-off Raman spectrometer for identification of liquids in a pressurized gas pipelines," Opt. Express **23**(3), 3027–3034 (2015).
13. N. R. Gomer, C. M. Gordon, P. Lucey, S. K. Sharma, J. C. Carter, and S. M. Angel, "Raman spectroscopy using a spatial heterodyne spectrometer: proof of concept," Appl. Spectrosc. **65**(8), 849–857 (2011).
14. K. A. Strange, K. C. Paul, and S. M. Angel, "Transmission Raman measurements using a spatial heterodyne Raman Spectrometer (SHRS)," Appl. Spectrosc. epub ahead of print (2016).
15. F. C. Thorley, K. J. Baldwin, D. C. Lee, and D. N. Batchelder, "Dependence of the Raman spectra of drug substances upon laser excitation," J. Raman Spectrosc. **37**(1-3), 335–341 (2006).

1. Introduction

In recent years there has been an increased interest in the use of Raman spectroscopy to monitor a variety of processes within industry [1–3]. Most commercial laser based spectrometers are designed to observe in a backscatter arrangement. The laser light is focused at the surface of a sample and the light emerging from the intercepted surface is recorded

#276221 http://dx.doi.org/10.1364/OE.25.001598
Journal © 2017 Received 30 Sep 2016; revised 15 Dec 2016; accepted 19 Dec 2016; published 19 Jan 2017

(Fig. 1). This can lead to errors if the sample is heterogeneous in nature [4]. Transmission Raman provides a bulk-average measurement of chemical compounds within a given sample [5,6] minimizing the influence of such samples. The technique is of significant interest to the security sector for the detection of counterfeit drugs [7] and the pharmaceutical sector for quality assurance observations [8].

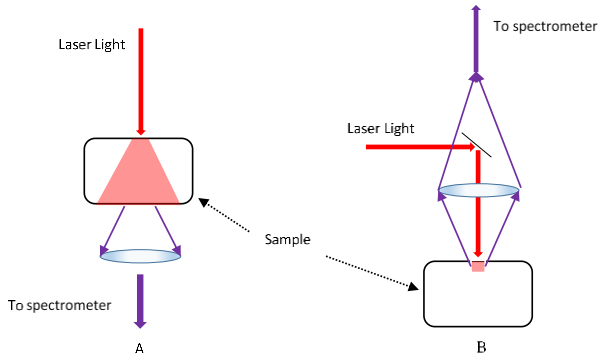

Fig. 1. Raman observational arrangements, impinging laser is shown by the red arrow, the scattering volume through the tablet is shown by the coloured area on the sample, the purple arrow shows the Raman photons being collected by the spectrometer, the two arrangements are: A = Transmission measurement setup; B = Backscatter measurement setup.

In a transmission Raman arrangement, the laser is fired at the target and allowed to disperse through the sample. The light exiting the sample on the opposite side is captured and measured (Fig. 1(a)). As the laser light propagates through the sample the Raman scattering is excited from the bulk of volume. The photons exit the sample from a large target area, often displaying Lambertian scattering properties. The light can be strongly attenuated by the sample, resulting in a weak Raman response [9]. The large etendue of the Raman light is a significant challenge for the analyzing spectrometer if the spectra are to be measured with sufficient resolution. Consequently, a significant fraction of the Raman light is lost, reducing the strength of the observed signal. This lack of signal has limited the development and use of Transmission Raman, in wider industry.

In a dispersive spectrometer the resolution is controlled by an entrance slit and its F number or NA, which limits the solid-angle area product, (AΩ or etendue) that can be accepted by the instrument. The resolution as a function of slit width is given by

$$\delta\lambda = \frac{RF\Delta\lambda W_s}{nW_p} \tag{1}$$

where Δλ is the spectral range of the spectrometer (which is a function of the imaging optics focal length), W_s is the slit width, n is the number of pixels and W_p is the pixel pitch, RF is the resolution factor. In order to distinguish to separate peaks at least three pixels are required Therefore best performance is achieved when $W_s \sim W_p$ which it can be shown gives a value of RF of 3.

To achieve a resolution of < 10 cm^{-1} with an excitation wavelength of 785 nm and a measurement range of 785- 920 nm, the slit width will typically be ≤ 50 μm in size, with a f/2 or slower collection lens, limiting the amount of light that can be collected. This has resulted in the development of fibre bundle based instruments. In these devices, a round bundle is presented at the target and a linear fibre stack at the spectrometer. These devices increase the etendue and can make the required observations, however they require more complex optical arrangements and can be expensive. Transmission Raman observations have also been made using Fourier transform spectrometers [10].

Optics EXPRESS

An alternative option is to use a Spatial Heterodyne Spectrometer (SHS), first described by Harlander et al (1992) [11]. The spectrometer has the configuration of a Michelson Interferometer but with the mirrors replaced by diffraction gratings (Fig. 2).

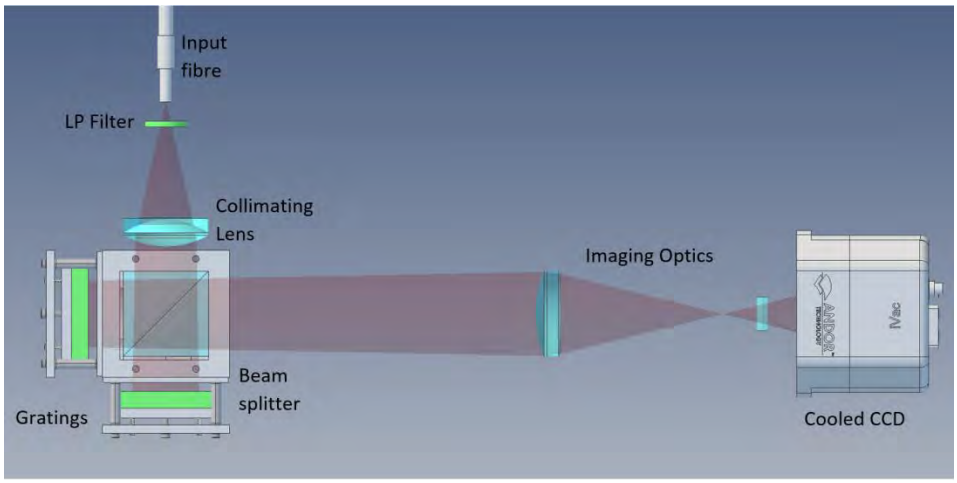

Fig. 2. A spatial heterodyne spectrometer arrangement.

The light that reflects from the gratings form an interference pattern which must be imaged onto a detector. The fringe pattern is Fourier Transformed to extract the spectrum of the received light. The instruments Field of View (FOV) and etendue are the same as a Fourier transform spectrometer [11],

$$\Omega = \frac{2\pi}{R} \tag{2}$$

where R is the instrument resolving power.

It can therefore be shown, for a given resolution a SHS can achieve a > 100-fold increase in etendue over a single fibre coupled dispersive device as described in detail by Harlander 1990 [12]. This, in principle, allows the instrument to collect light from a significantly larger sampling area, ideal for Transmission Raman measurements, maximizing the signal return. This in turn will lead to superior SNR or shorter integration times being required for a particular measurement. The instrument has no moving parts or expensive optical components, as required in FT-IR devices [12]. Spatial heterodyne systems have previously been used to make Raman measurements [13–15] however the throughput advantage that the design provides has not been fully exploited.

In this paper, a new spectrometer is described based on the SHS design, to fully exploit this inherent etendue advantage. The system has been designed to be fibre coupled and can accept light from fibres with core diameters of up to 3 mm and a numerical aperture (NA) of 0.22 (with no internal adjustment required).

2. Experimental configuration

A photograph of the assembled spectrometer is shown in Fig. 3. The system uses a cooled IVAC Front illuminated CCD (from Andor), and two reflective diffraction gratings with 60 lines per mm, 70 × 70 mm in size. The diameter illuminated at the grating was 40 mm giving a resolving power of 4800. Giving a measured single pixel resolution of 2.65 cm^{-1}.

Optics EXPRESS

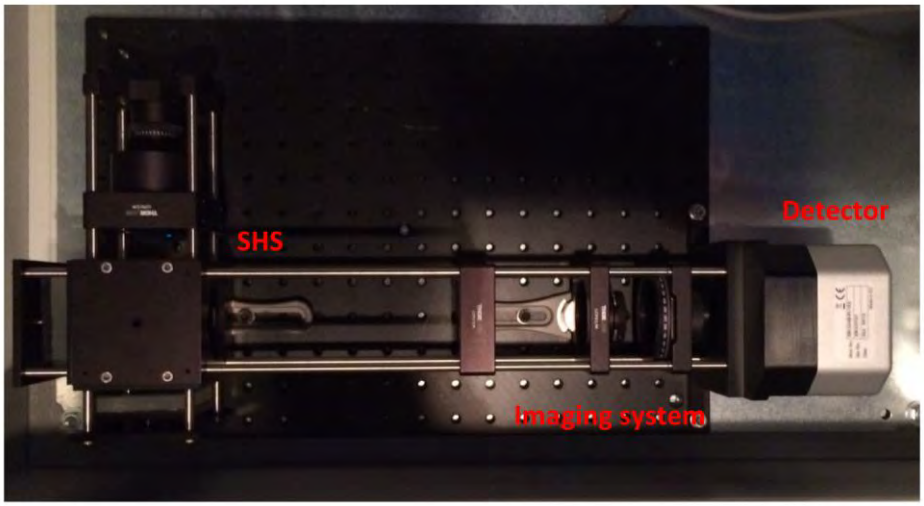

Fig. 3. The assembled spectrometer.

The laser was fibre coupled (PD-LD Blue Box supplied by Laser 2000), with an operating wavelength of 785 nm, with 500 mW of output power. The laser light was then passed through a 785 nm, 4 nm bandwidth clean up filter provided by Semrock (LL01-785-12.5), to eliminate any spontaneous emission from the laser. The laser power was measured after the fibre and filter was 150 mW. The schematic image of the sampling rig is given in Fig. 4.

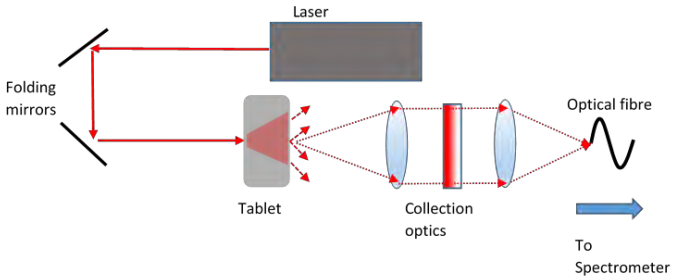

Fig. 4. Transmission Raman collection setup.

The measured sample was an approximately 5 mm thick paracetamol tablet. The light was collected by a matched pair of doublet lenses (focal length of 50 mm; diameter of 22 mm). Between the two lenses a Semrock 785 nm long pass filter (in addition to the filter mounted inside the spectrometer Fig. 2) was inserted to eliminate the laser light. The blocking level was better than 10^6, with the transmission of the filter being > 95% across the target range. The collected light was then focused into a variety of 0.22 NA fibers of different apertures. Each fiber was then in turn coupled to the spectrometer. The 2 mm and 3 mm diameter fibers were formed from bundles of 550 µm core fibers (7 and 19 respectively). The net collecting area of the fibre bundles being ~50% of the maximum that could be achieved, in both cases, when compared to a single core fiber. In addition, several 0.39 NA fibers were also tested with the system. However, given the coupling optics had a matched NA of 0.22, only the modes of the fiber associated with this NA were excited. All of the fibers were terminated with an SMA 905 with the exception of the 3 mm fibre bundle which required a custom ferrule termination. The complete range of fibres used for the experiment is given in Table 1.

Optics EXPRESS

Table 1. Optical fibres used in the experiment

Fibre dimeter (mm)	NA	Notes
0.05	0.22	
0.2	0.39	
0.4	0.39	
0.55	0.22	
0.6	0.22	
0.91	0.22	
1	0.39	
2	0.22	Bundle 7 × 550μm
3	0.22	Bundle 19 × 550μm

The experiment was repeated with a standoff backscatter configuration; the laser spot was focused to approximately a 1 mm diameter spot at the tablet. The collecting probe has a mono-axial configuration with a pair of F/2 lenses. The signal observed was significantly stronger than in the transmission Raman arrangement, thus the required integration times to record 3970 counts where approximately an order of magnitude lower for the smaller core diameter fibres.

3. Results

A transmission Raman spectrum was acquired from the paracetamol tablet using the 2 mm fiber bundle as the collection fiber (Fig. 5). The spectra are comparable to those obtained by previous authors [15]. The detector was used in a full vertical binning configuration with 3970 counts observed per pixel in the image. The integration time was 2.50 seconds. The observation was repeated 5 times to confirm its reproducibility. The fiber was then replaced in turn with each of those given in Table 1. The integration time was adjusted until 3970 counts per pixel was observed for each measurement and recorded. The spectrum showed excellent visual correlation for each of the fibres.

To quantify the differences observed a RMS deviation was computed for each spectrum with respect to the 2 mm fibre bundle observation. in the region 200–2000 cm-1 (normalized to the peak value) as a measure we note that the spectra deviated by no more than 2.7% except for two cases. The exceptions were the spectra taken with the 3 mm fiber bundle and the 50 μm core diameter fiber, which showed RMS deviations of 7.2 and 6.7% respectively. Figure 5 shows the observed spectra for the 50 μm, 2 mm and 3 mm fibers.

Optics EXPRESS

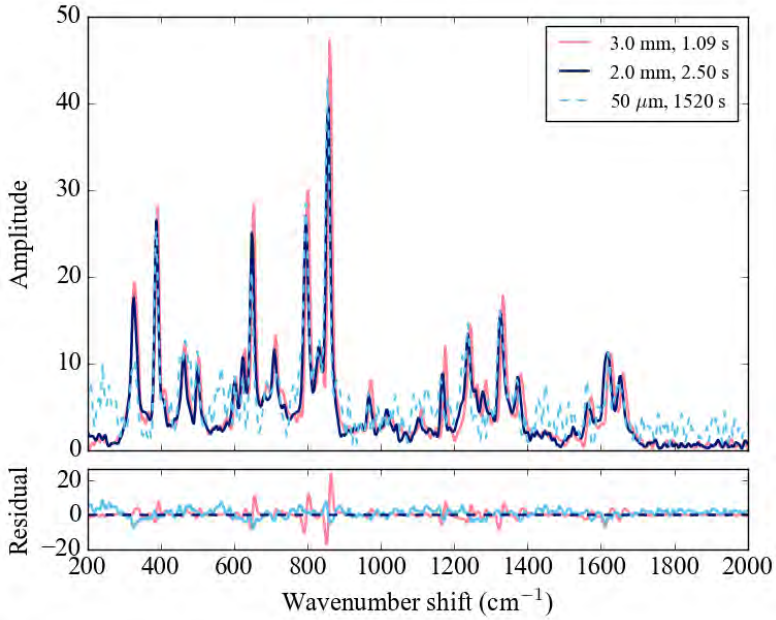

Fig. 5. Paracetamol Raman spectra when observed by the 50 μm core diameter fiber (dashed blue) as well as the 2 mm (solid dark blue) and 3 mm (solid orange) diameter fiber bundles. Plotted underneath is the residual or deviation between the 2 mm spectrum and the other two spectra: 3 mm (orange) and 50 μm (blue). The spectra taken with the 2 mm fiber bundle was taken as a standard, with the other spectra showing a normalized RMS deviation of 7.2 and 6.7% for the 3 mm and 50 μm fiber spectra. We can see from the spectra that the deviation is due to increased noise in the case of the 50 μm fiber spectra, while the deviation in the 3 mm case was due to a change in calibration when changing fiber adapters.

From inspection of the spectra in Fig. 5 we can see that the increased deviation in the case of the 3 mm fiber bundle is primarily due to a shift in calibration generated when the fiber adapter was changed. Correcting for this calibration change reduces the residue error to 2.8% (comparable to the other fibres). For 50 μm core fiber we can see that there is significantly more noise in the spectrum. This was due to the increased prominence of background light being observed (0.3 counts per pixel per second) and the required integration time being 1520 seconds.

The spectrum from paracetamol was also measured in a backscatter configuration, no change in its profile was observed. Figure 6 shows the required integration time to acquire the spectrum for both the standoff and Transmission Raman setups as a function of total fiber area. The observed Transmission Raman data is shown be the filled black circles. For comparison, the expected integration times for each fiber has been simulated by scaling the observed integration time for the 1 mm fibers proportionally to the area of the fiber at the collection rig, assuming the tablet sample is a perfect Lambertain scatterer with an area > 3 mm. These data are shown in Fig. 6 by the open black circles. The standoff observations are shown as open red circles, compared with simulated data shown as closed red circles.

Optics EXPRESS

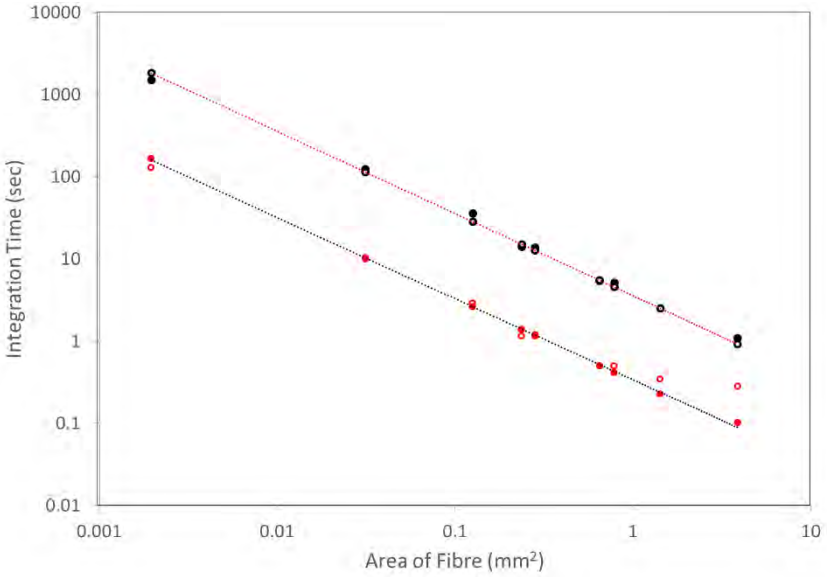

Fig. 6. Required integration time as a function of fiber area to observe 3970 photons per pixel with instrument in a Transmission (black) and standoff (red) configuration. Simulated (open circles) and observed data (filled circles).

The data for the Transmission Raman observations show an excellent correlation between the simulated and observed results for all of the fibres, demonstrating the spectrometer etendue advantage and ability to collect light from a fiber aperture up to 3 mm in diameter and that the tablet "glows" in a uniform Lambertain manner, with an area > 3 mm.

For the standoff Raman measurement, the correlation between the observed and simulated data diverge once the fibre diameter exceeds 0.91 mm. This divergence indicates that only marginal gains in terms of signal acquired are achieved with the larger fibres. This is due to the incident laser spot present on the sample is < 1mm in diameter and so only limited signal gain can be made.

4. Summary and conclusion

A new SHS spectrometer has been constructed compatible with a fiber input of up to 3 mm in diameter, with no slit being present within the spectrometer. The system performance and in particular its light throughput or etendue has been demonstrated in a transmission Raman configuration.

The results show that as the fiber aperture is increased so the amount of light gathered per unit time increases proportionally with the area of the collecting fiber. Crucially there is no observed loss of resolution when the fiber diameter is increased, demonstrating both the system's light gathering potential and the uniform Lambertian nature of the light exiting a sample when measured in a transmission Raman arrangement.

The system will have significant advantages in quality control applications and the detection of counterfeit drugs.